A solid carbon source based high performance mono/bi layer Graphene/SiNWs heterojunction NIR photodetector

Harsh A. Chaliyawala[1], Zeel Purohit[2], Neha Agarwal[3], Govind Gupta[3], Abhijit Ray[1], Indrajit Mukhopadhyay[*1]

[1]Solar Research and Development Center, Department of Solar Energy, Pandit Deendayal Petroleum University, Raisan, Gandhinagar- 382421, Gujarat, India.

[2]Department of Physics, School of Technology, Pandit Deendayal Petroleum University, Raisan, Gandhinagar-382421, Gujarat, India

[3]Thin Film Devices Group, CSIR-National Physical Laboratories, Dr. K.S. Krishnan Marg, New Delhi-110 012, India.

ABSTRACT

Semiconductor nanowires, especially Si nanowires (SiNWs) have attracted much attention due to its high broadband absorption, high density and extra ordinary surface/volume ratio. Moreover, nanowires are ideal candidates for light detection, large responsivity, a fast response speed, and an excellent detection limit. These opto-physical properties demonstrates their high potential for practical applications in advanced devices such as transistors, photodetectors, light-emitting-diodes, solar cells, bio/chemical sensors, and etc. Graphene on the other hand, exhibits an extremely high charge carrier mobility, a very broad spectral range of detection from ultraviolet to terahertz and quasi wavelength independent absorption, which is a result of its gapless band nature. Compatibility of Graphene with Si or SiNWs makes it a promising candidate for large-scale and cost effective ultrafast photodetection. The growth of high-quality CVD graphene from camphor and its high performance optical device has not been addressed so far. We have presented high performance near infrared photodetectors (NIRPDs) by using camphor as solid source of carbon for developing mono-bi layer Gr/SiNW arrays schottky heterojunction. The nanowire arrays shows excellent optical light trapping properties and on the other hand, graphene act as transparent conductive metal sheet. Hence a combination of graphene over SiNWs serves as an excellent NIR light coupling system. The as-prepared device has also shown remarkable responsivity from μA/W to mA/W at 0 V bias, for Gr/Si and Gr/SiNWs heterojunction, respectively. On the other hand, as prepared device shows excellent responsivity upto 2V bias, which suggests that our approach to make graphene sheet by natural camphor will have a potential application to make self-driven low bias NIRPDs in future optoelectronic devices.

Keywords: Si nanowires; Graphene; Atmospheric chemical vapor deposition (APCVD) process; near infrared photodetectors; metal assisted electroless chemical etching (MACE); Schottky heterojunction.

1. INTRODUCTION

A two-dimensional layer of carbon atoms known as Graphene consists of a unique band structure and its tunable work function, has recently attracted much interest in photonic applications such as sensors[1], polarizer[2], modulator[3], transparent electrodes[4], surface plasmonic device (SPs)[5], surface plasmon polaritons (SPPs), solar cells[6] and photodetectors (PDs)[7]. In addition, one of the most impressive advantages is its ability to absorb 2.3% of incident light over a broad wavelength range regardless of its one-atom layer thickness. This extra-ordinary advantage makes the realization of broadband photodetectors possible, far exceeding the bandwidth of the existing photodetectors[7].

Silicon (Si) on the other hand, with its indirect narrow band gap (~1.12 eV) is a key material for nano-electronic industry. As compared to its bulk and thin film structures, vertical Si nanowire arrays (SiNWs) with its large surface to volume ratio, strong light trapping ability and superior electron transport properties, has shown a tremendous potential as a building block for various optoelectronic devices such as field effect transistors (FETs)[8], solar cells[9], sensors[10] and photodetectors[11,12]. Among various operational nanoscale devices, SiNWs based PDs has received special research interest due to its ability to probe incoming infrared light with high sensitivity and excellent photo response, which can have a

[*] Correspondence: indrajit.m@sse.pdpu.ac.in, phone no: +91-9586864936.

Optical Sensors 2019, edited by Francesco Baldini, Jiri Homola, Robert A. Lieberman, Proc. of SPIE Vol. 11028, 1102803 · © 2019 SPIE · CCC code: 0277-786X/19/$18 · doi: 10.1117/12.2522581

future component for large scale applications in military surveillance, target detection and tracking[13]. In order to exhibit the extraordinary properties of both the materials, recent research interests lies to combine vertical SiNWs with graphene sheet, to construct high-performance energy selective metal/semiconductor Schottky heterojunction photodetectors. Till now Gr/Si based Schottky junction solar cells[14] and photodetectors[15] have been introduced by showing chemical vapor deposition (CVD) graphene synthesis by methane as a main precursor. Since last decades, researchers have shown the progress in graphene film from solid precursor, which can be much more suitable and alternative approach for CVD process rather than using common and toxic gas sources as a carbon precursors such as methane[16-19]. Among all precursors, Camphor as an alternative green botanical source of carbon has been employed by few of the research groups all around the globe[20-24]. Few reports show the study on developing large single crystal graphene film by using camphor as a source on various substrates such as Ni, Cu foil etc. at various temperature conditions but did not get ahead to fabricate a device by camphor route[22,23,25-27]. To the best of our knowledge, there are no such reports till now on development of a highly sensitive and self-driven near infra-red photodetectors (NIRPDs) by using camphor as a source for Graphene/SiNWs schottky heterojunction device. Herein, we have proposed a very first high performance SiNWs based NIRPDs by exhibiting a facile and novel approach of making mono/bi-layer Graphene by camphor as a source of carbon. The as-fabricated device is sensitive to 940 nm infrared radiation, with highest ON/OFF ratio of 10^6, as comparable with the Si based devices. The nanowire arrays show excellent optical light trapping properties and on the other hand Graphene act as transparent conductive metal sheet together serves as an excellent NIR light coupling system. The as-prepared device has also shown remarkably good performance at 0 V bias, which suggests that our approach to make graphene sheet by natural camphor for developing SiNWs based NIRPDs will have a potential application in future optoelectronic devices.

2. EXPERIMENTAL PROCEDURE

2.1 Preparation of SiNWs and graphene

The SiNWs in the present work was fabricated by employing a very facile Ag assisted electroless etching technique. In brief, 1 cm^2 Si samples (ρ =1-10 Ω cm) were thermally oxidized at 1000°C for 4 h under O_2 atmosphere to form 200 nm SiO_2/n-Si substrates. Hereafter, an active area of 0.3 x 0.3 cm^2 were decided on n-Si (100) wafers. The buffer oxide etch solution (BOE, NH_4F/HF; 6:1) was further used for SiO_2 etching, to expose a chosen active window by masking the remaining area by adhesive tape for the device fabrication. The as-obtained substrate was then immersed in an aqueous solution of HF (4.8M) and $AgNO_3$ (5mM) to coat AgNPs, which will act as a catalyst for further process. The Ag active Si surface was then immersed in a mixture of HF (40%) and H_2O_2 (30%) aqueous solutions for few minutes to obtain vertically aligned SiNWs. Finally, the residual AgNPs on as-obtained SiNWs were soaked in an aqueous HNO3 solution (in the ratio of 10:1 using 50%w/v HNO_3), cleaned with deionized water and dried at room temperature in natural air. Mono/bi-layer graphene sheet was grown on 25 μm Cu foil at 1020 °C by using natural camphor (3.5 mg) as a solid source via atmospheric chemical vapour deposition method (APCVD). After growth, the Cu coated graphene sheet was spin coated with polymethylmethacrylate (PMMA) in chlorobenzene, and finally the underneath Cu foil was removed by using ammonium per-oxodisulfate ($(NH_4)_2S_2O_8$) as a Cu etchant solution. After, Cu etching, the PMMA coated graphene sheet were rinsed 5 times in a DI water by lift-off process. Finally, graphene coated PMMA was transferred on to the n-SiNWs in the active area window and PMMA was removed by acetone.

2.2 Device assembly

To fabricate the graphene/SiNWs Schottky junction photodetector, nanowire arrays which serves as an active layer on SiO2/Si wafers were first fabricated using electroless etching technique. Hereafter, PMMA coated graphene sheet was directly transferred on the top of SiNWs. The samples were kept under vacuum for 24 h and then residual PMMA was removed by acetone rigorously. Ag as an electrode was pasted on the front side and rear side of the Si substrate to achieve an ohmic contact.

2.3 Characterization techniques involved

Surface morphological study for vertical SiNWs were investigated by field emission scanning electron microscopy FE-SEM (Zeiss, Ultra-55) equipped with EDX (Oxford Instruments). The optical study has been recorded using a UV-Vis (UV-2600, Shimadzu) spectrophotometer in a wide range of 200-1400 nm equipped with an integrating sphere. Micro Raman measurements has been carried out using (Renishaw inVia system) with an excitation laser beam focused at 532 nm to identify the crystallinity, defects states and the number of layers of graphene. The device characterization of mono/bi-layer graphene/SiNWs were measured under solar simulator (SS80AAA, Photoemission Tech., USA) equipped with

AM1.5G filter and source measuring unit (U2722A, Agilent) by applying the bias of -1 to +1 V. The photoresponse measurements were carried out in the probe station which was equipped with a lamp source (190 nm – 2200 nm) for detection and a source meter (Keithley 2450) Unit. X-ray Photoelectron Spectroscopic measurements for one of the graphene transferred on Si samples were performed in multiprobe surface analysis (Scienta Omicron, Germany) using monochromatized Al Kα (1486.7 eV) radiation source. The pass energy of the scans was kept at 20 eV with an ultimate spectral resolution of ~0.02 eV. The transmission electron microscopic analysis (JEOL 2100) was conducted at 200 KeV with a point to point resolution of 0.19 nm. Graphene samples were successfully transferred on the carbon coated Cu grid by standard transfer method process.

3. RESULTS AND DISCUSSION

The surface of as-grown SiNWs as shown in Fig. 1 (a), indicates the formation of a highly dense and confined nanowire structure. These highly random nanostructure on the surface can work as an effective path for the light to get trapped inside the cavity of nanowires. As shown in Fig. 1 (b), cross sectional FESEM images indicates that SiNWs are vertically aligned and well inter connected in (100) orientation with typical length of about ~10 µm. On the other hand, Fig. 1 (c) depicts the

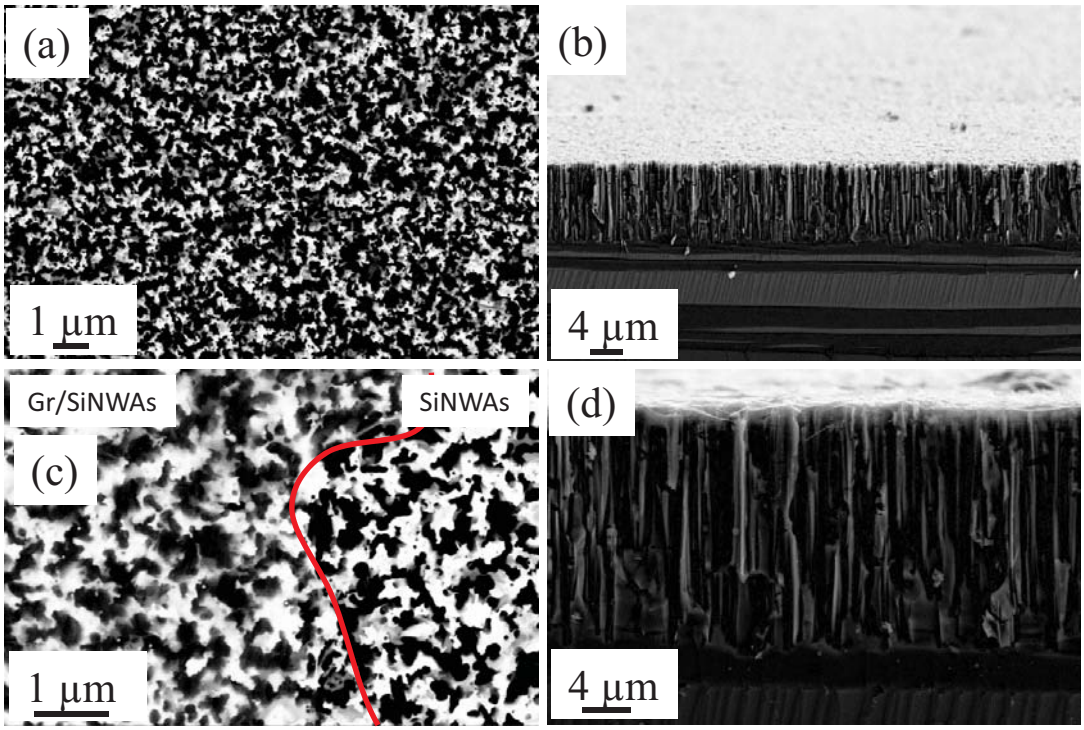

Figure 1: (a) Surface morphology of the as etched SiNWs indicating highly dense structure; (b) surface cross sectional image of highly dense SiNWs; (c) demonstrates a cross-sectional view of graphene covered on top of the vertical SiNWs and (d) shows the mono/bi-layer graphene on the tip of SiNWs.

surface profile of graphene sheet as observed on the top of nanowire arrays with a difference in two regions. The camphor grown mono/bi-layer graphene sheet has been transferred on the top of SiNWs to act as a transparent conductive sheet for the development of NIRPDs. The cross-sectional FESEM image as seen in Fig. 1 (d), clearly shows a fully covered transparent conductive graphene sheet on the top of SiNWs, which possess higher transparency leading to maximize more light absorption and increases carrier transport mechanism of the device[28-30]. A homogeneous formation and island growth of mono/bi- layer graphene sheet is very well connected over the SiNWs to function as a transparent conductive sheet on a semiconductor tip surface.

From Fig. 2 (a), it has been observed that about 35-40 % of incident light is reflected back at the interface. Interestingly, when the incoming light interacts at the interface of the nanowire arrays, a tremendous reduction in reflectance upto 4% has been observed over a whole visible to near-IR regime due to its effective light trapping properties as discussed in our earlier reports [31-33]. On the other hand, Fig. 2 (b) presents the transmittance spectra of graphene sheets transferred on glass

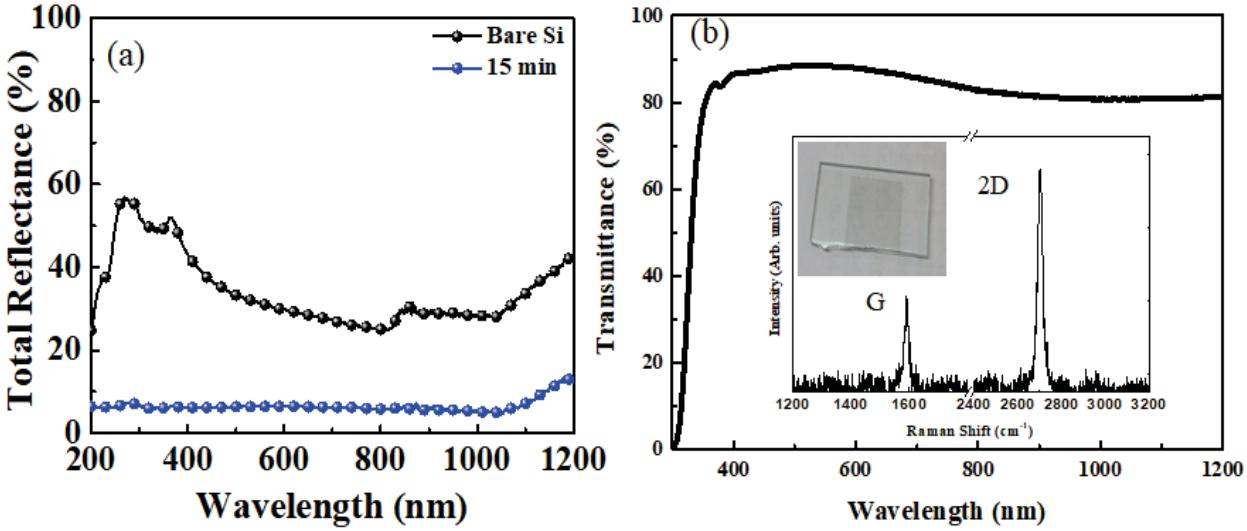

Figure 2: (a) Shows the optical Reflectance spectra of planar Si and Si nanowires grown for 15 min over a wide range of 200-1200 nm; and (b) shows the transmittance spectra of mono/bi- layer graphene sheet transferred on soda lime glass substrates. Moreover, the inset of Fig. 2 (b), represents the Raman spectra of mono/bi-layer graphene sheet by using camphor as a carbon source. The inset also shows an optical image of graphene transferred on a glass substrate.

substrate in the wide range of 300-1200 nm regime. The maximum transmittance value 84.4% has been achieved for mono/bi layer graphene at 550 nm. The inset of Fig. 2 (b) demonstrates an optical image for graphene transferred on glass substrates, which clearly indicates a very high transparency of graphene sheet. In addition, the inset of Fig. 2 (b) represents a micro Raman spectra, taken at various regions to determine the uniformity and the surface defects of the as-grown graphene sheet. It is observed that, there are two sharp peaks at ~2689 cm^{-1} and ~1598 cm^{-1}, which are the characteristic 2D and G band of graphene sheet. The intensity ratio of 2D:G = 1.40, respectively, suggests that camphor grown graphene is monolayer at most of the places with a presence of few defects[20,26,27]. In order to understand the chemical states of mono-bi layer graphene sheet XPS study has been carried out as shown in Fig. 3 (a). The core level peak of the C1s is determined into three major components corresponding to carbon atoms at different chemical environments. The convoluted peak consisting of two broad peaks at binding energy 284.7 eV and 285.2 eV. The sharp peak at binding energy 284.7 eV

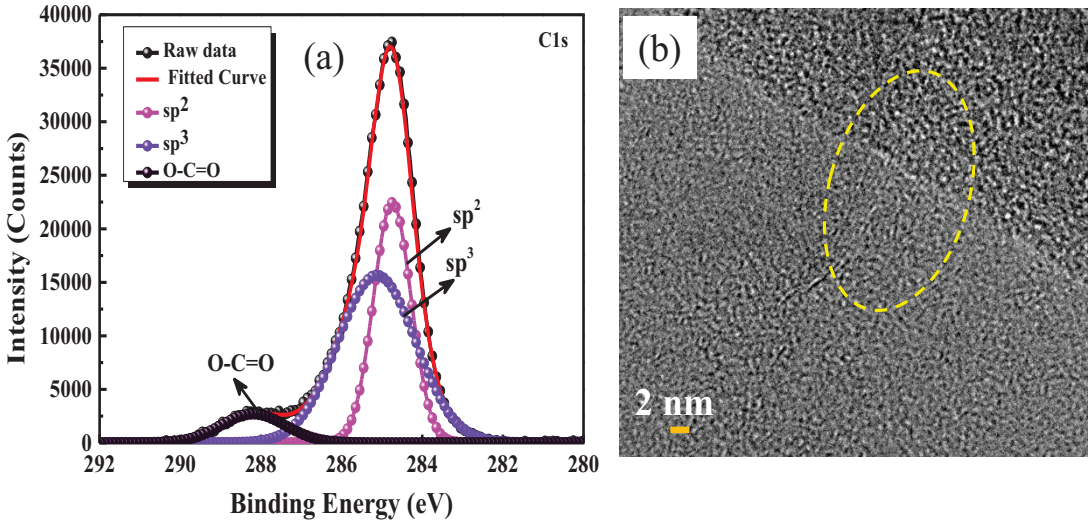

Figure 3: (a) Represents the XPS core level spectra of C 1s for graphene sheet and (b) represents the HRTEM images for graphene sheet transferred on carbon coated TEM grid.

represents graphitic carbon i.e. sp2 hybridized while the characteristic feature attributed to the presence of defects states

i.e. sp3 hybridized is observed at 285.2 eV [34-36,27]. The break in the ring of resonating aromatic carbon bonds maybe the additional reason for the existence of such a broad defect peak. Moreover, the oxidized states of carbon (C_{ox}) are also observed at 288.3 eV. Moreover, Fig. 3 (b) presents the HRTEM images of a graphene samples grown from camphor to identify the number of layers and to support the Raman observations. The edge of the graphene film that folds back and allows us to identify the cross-sectional view of graphene sheet. It is evident to observe the existence of single layer graphene by camphor as highlighted in the yellow circle which is similar with the existing literatures [21, 23, 37, 38].

The work mechanism of the camphor driven Gr/Si and Gr/SiNWs devices, photovoltaic and photoresponse characteristics have been investigated as shown in Fig. 4. The scheme shows a Gr/SiNWs schottky heterojunction device

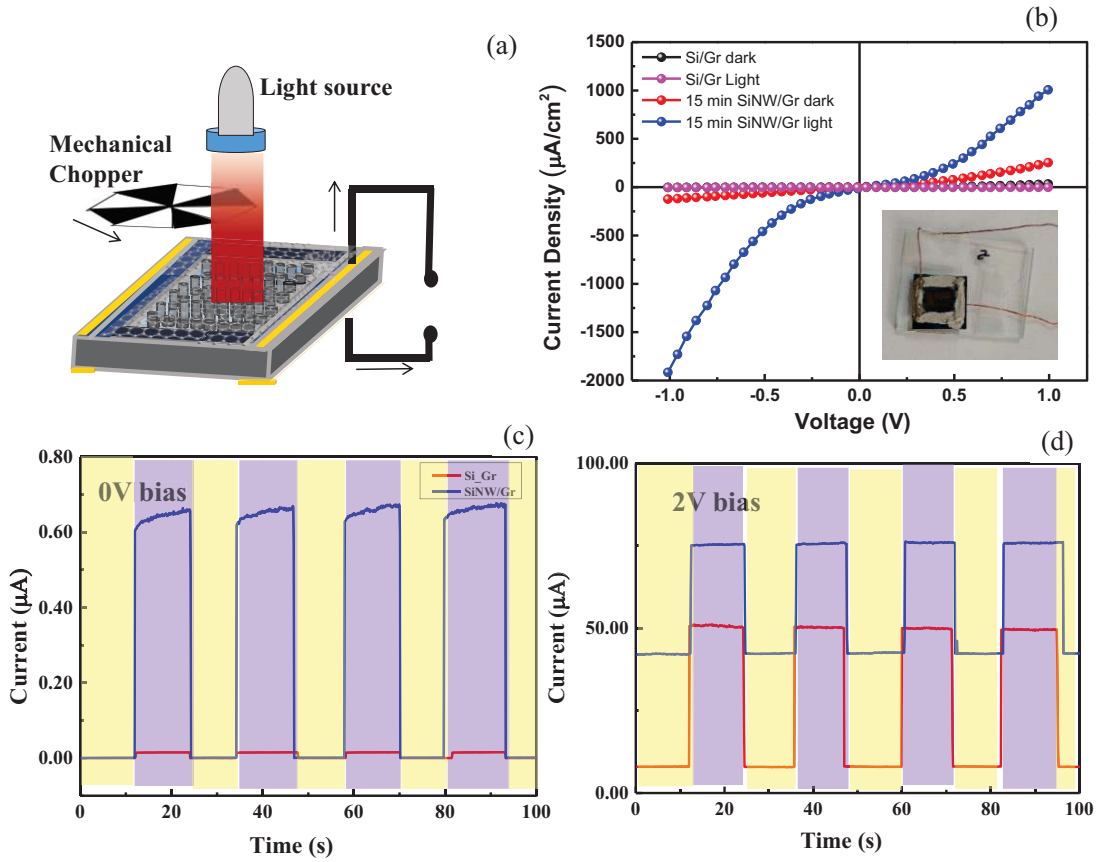

Figure 4: (a) Represents the scheme of Gr/SiNWs devices under NIR light with a mechanical chopper; (b) displays the J-V curve of Gr/Si and Gr/15 min SiNWs PDs under dark and illumination condition; (c) and (d) shows the photoresponse behavior at different bias of 0V and 2V of as mentioned devices.

in Fig. 4 (a) with front and back Ag metal contacts, connected externally by a source meter. As seen SiNWs are embedded inside a transparent metal conducting graphene sheet. Fig. 4 (b) represents a typical dark and light current-voltage (*J-V*) curve of Gr/Si schottky junction NIRPDs device. The excellent rectifying behavior has been observed due to the formation of the schottky barrier. It is also observed that, the Gr/Si exhibit very less dark current; whereas as the current increases in the case of Gr/15 min SiNWs device. Under illumination condition, it is seen that these devices exhibit pronounced rectification and photovoltaic effect upon incident radiation of 1000 W/cm^2. Moreover, J_{SC} value increases from 2.8 μA/cm^2 to 11.4 μA/cm^2 for Gr/15 min SiNWs devices at the expense of Gr/Si NIRPDs. This enhancement indicates that nanowires which can now trap the light, shows an extreme support in the enhancement of current transport mechanism. The inset of Fig. 4 (b), depicts the optical image of the as-fabricated Gr/SiNWs NIRPDs by using camphor as a carbon source. Furthermore, the time-dependent photoresponse measurements were carried out at different bias variation from V_{bias} = 0, 1 and 2 V. Fig. 4 (c) demonstrates the photocurrent measurement at 0V bias for Gr/Si, Gr/15 min SiNWs devices, respectively. When the light was turned ON and OFF alternatively at V_{bias} = 0 V, Gr/Si devices shows a minimum dark current of (I_{dark}) 0.1 pA and a maximum light current (I_{light}) of 0.01μA. Interestingly, the 15 min Gr/SiNWs devices shows

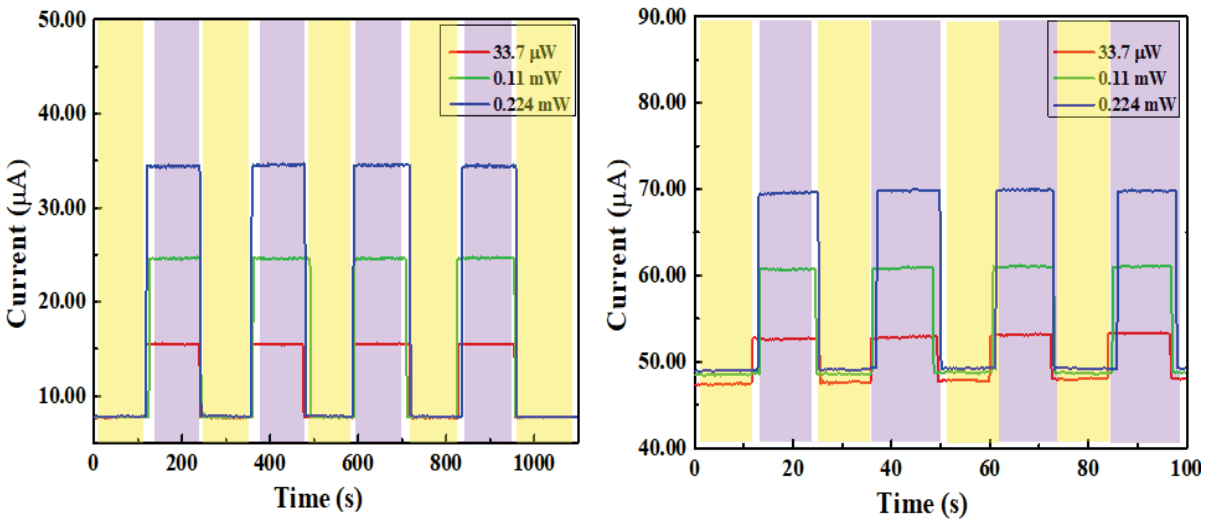

Figure 5: Represents the photoresponse behavior at various power intensity variation for (a) Gr/Si and (b) Gr/15 min SiNWs under 2V bias conditions, respectively.

a tremendous increase in a photocurrent; with a minimum dark current of (I_{dark}) 5.5 x 10^{-4} μA, and a maximum light current (I_{light}) of 0.6 μA, which yields to a high I_{light}/I_{dark} ratio ≥ 10^3. This high current under illumination can be attributed to the maximum absorption of the vertically aligned nanowires which is not in the case of Gr/Si devices, and also due the conductivity of mono/bi-layer graphene sheet that supports to enhance and conducts the electron flow into the circuit. Moreover, the devices are highly reversible in the sense that electron and holes can be effectively separated and generated, which facilitates to show a large current at 0 bias, yielding a self-driven capability of the devices. As we apply voltage of V_{bias} = 2 V, there is a tremendous enhancement in the photocurrent for the Gr/15 min SiNWs devices as compare to Gr/Si devices. The photocurrent current is even more than in the case of no bias condition as seen from Fig. 4(d). For instance, at V_{bias} =2 V, when the light was turned ON and OFF alternatively the increment in light current I_{light} is found to be 50 μA and 75 μA for Gr/Si and Gr/15 min SiNWs, respectively. This enhancement shows that the devices can delivers more current at a typical applied bias voltages. It is to be noted that, at high bias voltages the dark current also increases tremendously due to high surface recombination at the nanowire/Gr interface, which is not appropriate for a stability of the device.

Various performance parameters of photodetectors have been calculated to compare the results for the fabricated

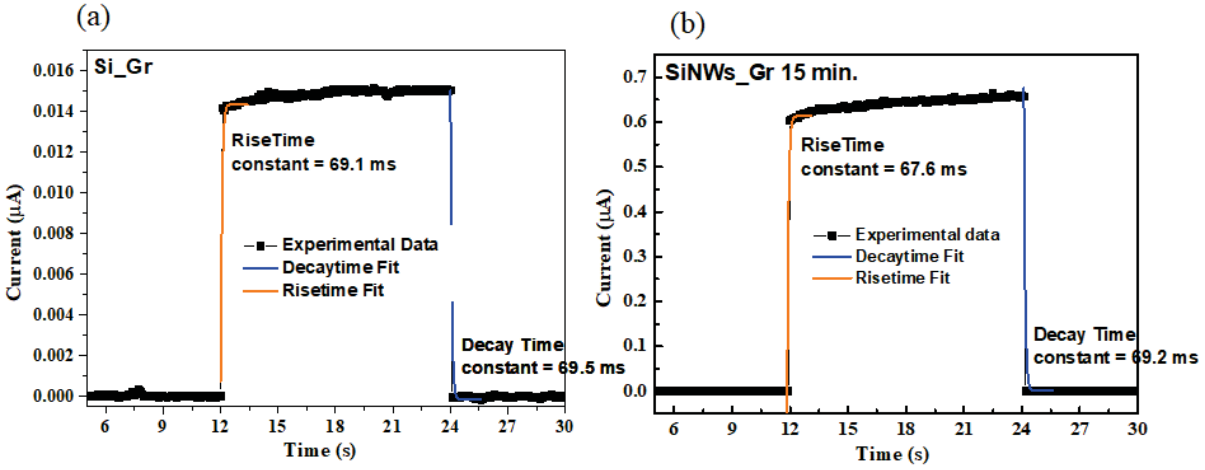

Figure 6: displays the fitted curve for rise and decay time constants for (a) Gr/Si and (b) 15 min Gr/SiNWs NIRPDs acquired at maximum power of 0.4 mW under 0 V bias.

devices for 0V and 2V bias variation as shown in table 1. It is to be noted that all the devices response quite well and are

more sensitive at 940 nm. The responsivity (R), Detectivity (D) and noise equivalent power (NEP) quantify the ability of a photodetection device to be responsive towards a particular optical signal and is given by[13],

$$R = \frac{I_{ph}}{P_{in} * A} \quad (1)$$

$$D = R * \sqrt{\frac{A}{2 * e * I_d}} \quad (2)$$

$$NEP = \frac{\sqrt{2 * e * I_d}}{R} \quad (3)$$

Where R = responsivity of device, D= detectivity, I_{ph}= measured photocurrent (I_{light} - I_{dark}), P_{in} = incident optical power in (mW), e = electronic charge, I_d = dark current and A = active area of the respected devices (A = 0.09 cm^2). The responsivity increases in the order of 10^3 for Gr/15 min SiNWs device at 0 V bias. Moreover, the detectivity has also been significantly increased and found to be in the order of ~10^{12}. Fig. 5 represents the photoresponse measurements for Gr/Si and Gr/15 min SiNWs under illumination with various power intensities. It is evident from Fig. 5 (a) and (b) that, when the switching is performed at various power intensities (from ~33.7 µW to 0.4 mW) of the optical signal, there is a clear enhancement in the photocorrelated response and shows a good sensitivity with increasing power intensity[12,13,36]. Fig. 6 displays the fitted curve for rise and decay time constants for Gr/Si and Gr/15 min SiNWs NIRPDs acquired at maximum power of 0.4 mW under 0 V bias. The rise time constant for Gr/Si and Gr/15 min SiNWs is 69.1 ms and 67.6 ms, respectively. This clearly indicates, that the switching action of Gr/15 min SiNWs is faster as compared to Gr/Si NIRPDs.

Table 1: Various calculated photoresponse parameters for Gr/Si and Gr/15 min SiNWs devices.

Device	Responsivity (A/W)		I_{light}/I_{dark}		Detectivity (Jones)		Noise Equivalent power (NEP) (x 10^{-12} W $(Hz)^{-1/2}$)	
	0V Bias	2V Bias	0V Bias	2V Bias	0V Bias	2V Bias	0V Bias	2V Bias
Gr/Si	36.7 x 10^{-6}	1.12	~10^3	~10^1	4.5 x 10^9	2.0 x 10^{12}	161.6	1.39
15 min Gr/SiNWs	16.4 x 10^{-3}	0.88	~10^3	~10^0	3.4x 10^{12}	7.3 x 10^{11}	0.82	4.16

Fig. 7 (a) shows the comparison of Gr/Si and Gr/15 min SiNWs NIRPDs to evaluate the effect on responsivity associated to the representative devices at various optical power intensities. Evidently, R value decreases as the power increases from Eq. (1), but it is important to notice that even for lower power intensity the R value is ~1.68 A/W for Gr/15 min SiNWs which is very high as compared to 2.69 A/W for Gr/Si NIRPDs.

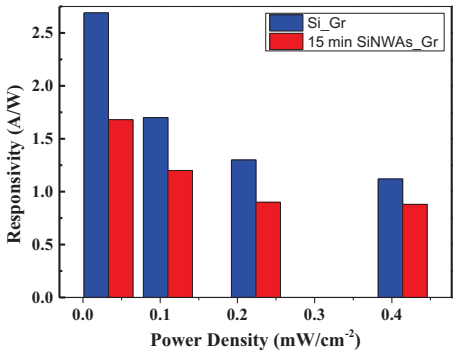

Figure 7: Represents the effect of power on responsivity for Gr/Si and 15 min Gr/SiNWs NIRPDs acquired at maximum power of 0.4 mW under 2 V bias.

4. CONCLUSION

In summary, high performance NIRPDs have been successfully fabricated by using a very facile camphor based mono/bi layer graphene sheet spreaded on n-Si and on SiNWs. A systematic study has been performed to realize the self-driven NIRPDs with a novel synthesis of graphene on n-Si and Si nanowire arrays substrates. Device with planar n-Gr/Si and Gr/15 min SiNWs shows a pronounced photovoltaic behavior under illumination condition. The optimization of maximum absorption capability of nanowire arrays and an increase in surface recombination centers leads to the maximum JSC of ~ 11.8 $\mu A/cm^2$ for Gr/15 min SiNWs PDs. Moreover, device analysis shows that Gr/15 min SiNWs PDs can work with high response speed with 67/69 ms and very low NEP of 0.82 pW $(Hz)^{-1/2}$ at the expense of planar Gr/Si devices. Therefore, a facile fabrication process of synthesizing graphene from camphor can lead to a remarkable low cost photodetectors and makes it a promising candidate for future high-performance SiNWs based NIRPDs.

5. ACKNOWLEDGEMENT

The authors would like to thank Council for Scientific and Industrial Research (CSIR) for awarding CSIR-Senior Research Fellow (SRF) fellowship. Authors also thank Pandit Deendayal Petroleum University (PDPU) for providing the necessary facilities to carry out this investigation. Financial support from Solar Research and Development Center (SRDC), PDPU is deeply acknowledged.

Conflict of Interest

The authors declare no conflict of interest.

Author Information:

Email id: indrajit.m@sse.pdpu.ac.in,

6. REFERENCES

[1] J. Kim, S. Oh, J. Kim, D. Shin, S. Kim, S. Choi, Scientific Reports 2014, 4.

[2] Q. Bao, H. Zhang, B. Wang, Z. Ni, C. Lim, Y. Wang, D. Tang, K. Loh, Nature Photonics 2011, 5.

[3] G. Kovacevic, C. Phare, S. Set, M. Lipson, S. Yamashita, Applied Physics Express2018, 11.

[4] J. Shen, X. Liu, X. Song, X. Li, J. Wang, Q. Zhou, S. Luo, W. Feng, S. Lu, S. feng, X. Wei, C. Du, Y. Wang, H. Shi and D. Wei, Nanoscale, 2017,9, 6020-6025.

[5] Q. Zhang, X. Li, M. Hossain, Y. Xue, J. Zhang, J. Song, J. Liu, M. Turner, S. Fan, Q. Bao, M. Gu, Scientific Reports 2014, 4.

[6] T. Echtermeyer, S. Milana, U. Sassi, A. Eiden, M. Wu, E. Lidorikis, A. Ferrari, Nano Letters 2015, 16.

[7] B. Zhang, T. Liu, B. Meng, X. Li, G. Liang, X. Hu, Q. Wang, Nature Communications 2013, 4.

[8] M. Gautam, A. Jayatissa, Journal of Applied Physics 2012, 112.

[9] C. Xie, P. Lv, B. Nie, J. Jie, X. Zhang, Z. Wang, P. Jiang, Z. Hu, L. Luo, Z. Zhu, L. Wang, C. Wu, Applied Physics Letters 2011, 99.

[10] X. An, F. Liu, Y. Jung, S. Kar, Nano Letters 2013, 13.

[11] P. Gowda, D. Mohapatra, A. Misra, ACS Applied Materials & Interfaces 2014, 6.

[12] P. Gowda, T. Sakorikar, S. Reddy, D. Ferry, A. Misra, ACS Applied Materials & Interfaces 2014, 6.

[13] L. Luo, L. Zeng, C. Xie, Y. Yu, F. Liang, C. Wu, L. Wang, J. Hu, Scientific Reports2014, 4.

[14] X. Li, H. Zhu, K. Wang, A. Cao, J. Wei, C. Li, Y. Jia, Z. Li, X. Li, D. Wu, Advanced Materials 2010, 22.

[15] S. Riazimehr, A. Bablich, D. Schneider, S. Kataria, V. Passi, C. Yim, G. Duesberg, M. Lemme, Solid-State Electronics 2016, 115.

[16] Z. Sun, Z. Yan, J. Yao, E. Beitler, Y. Zhu, J. Tour, Nature 2010, 468.

[17] T. Liang, Y. Kong, H. Chen, M. Xu, Chinese Journal of Chemistry 2015, 34.

[18] G. Kalita, T. Sugiura, Y. Wakamatsu, R. Hirano, M. Tanemura, Royal Society Of Chemical 2014, 4.

[19] G. Kalita, R. Hirano, M. Ayhan, M. Tanemura, Journal of Physics D: Applied Physics 2013, 46.

[20] G. Kalita, K. Wakita, M. Umeno, Physica E: Low-dimensional Systems and Nanostructures 2011, 43.

[21] F. Ravani, K. Papagelis, V. Dracopoulos, J. Parthenios, K. Dassios, A. Siokou, C. Galiotis, Thin Solid Films 2013, 527.

[22] G. Kalita, M. Masahiro, H. Uchida, K. Wakita, M. Umeno, Materials Letters 2010, 64.

[23] S. Sharma, G. Kalita, R. Hirano, Y. Hayashi, M. Tanemura, Materials Letters2013, 93.

[24] P. Somani, S. Somani, M. Umeno, Chemical Physics Letters 2006, 430.

[25] K. Sharma, S. Shinde, M. Rosmi, S. Sharma, G. Kalita, M. Tanemura, Journal of Materials Science 2016, 51.

[26] S. Shinde, E. Kano, G. Kalita, M. Takeguchi, A. Hashimoto, M. Tanemura, Carbon 2016, 96.

[27] G. Kalita, S. Sharma, K. Wakita, M. Umeno, Y. Hayashi, M. Tanemura, physica status solidi (a) 2012, 209.

[28] X. Zhang, C. Xie, J. Jie, X. Zhang, Y. Wu, W. Zhang, Journal of Materials Chemistry A 2013, 1.

[29] Y. Wu, X. Zhang, J. Jie, C. Xie, X. Zhang, B. Sun, Y. Wang, P. Gao, The Journal of Physical Chemistry C 2013, 117.

[30] G. Fan, H. Zhu, K. Wang, J. Wei, X. Li, Q. Shu, N. Guo, D. Wu, ACS Applied Materials & Interfaces 2011, 3.

[31] H. Chaliyawala, Z. Purohit, S. Khanna, A. Ray, R. Pati, I. Mukhopadhyay, Journal of Applied Physics 2018, 123.

[32] H. Chaliyawala, Z. Purohit, S. Khanna, A. Ray, R. Pati, I. Mukhopadhyay, Nanotechnology 2019, 30.

[33] H. Chaliyawala, A. Ray, R. Pati, I. Mukhopadhyay, Optical Materials 2017, 73.

[34] S. Botti, A. Rufoloni, A. Vannozzi, and Stefano Gay, AIP Conference Proceedings 2018, 1990, 020007 (1)-(6).

[35] Z. Tu, Z. Liu, Y. Li, F. Yang, L. Zhang, Z. Zhao, C. Xu, S. Wu, H. Liu, H. Yang, P. Richard, Carbon 2014, 73, 252-258.

[36] B. Lesiak, L. Stobinski, A. Malolepszy, M. Mazurkiewicz, L. Kövér and J. Tóth, J. of Electron Spectrosco. Related Phenomena 193 (2014) 92–99.

[37] W. Regan, N. Alem, B. Alemán, B. Geng, Ç. Girit, L. Maserati, F. Wang, M. Crommie, A. Zettl, Appl. Phys. Lett. 2010, 96, 113102.

[38] E. Moreau, F. Ferrer, D. Vignaud, S. Godey, X. Wallart, physica status solidi (a) 2010, 207, 300-303.